Creep Analysis of Hybrid Integral Bridges

K. A. SIROS AND C. C. SPYRAKOS

A state-of-the-art three-dimensional (3-D) model is developed and utilized for nonlinear creep analysis of composite (steel stringer-concrete slab) integral bridges. The results of the analysis are evaluated and compared with results of an equivalent two-dimensional (2-D) linear creep analysis. The rate of creep method and the age-adjusted effective modulus method are employed for the 3-D and the 2-D analysis, respectively. Two typical structural systems are analyzed: a single-span bridge (15.24 m) and a two-span bridge (2 × 34.75 m). Change of stresses with time at critical points of the bridges are shown and comparisons of the 2-D and the 3-D analyses are included. Evaluation of the results with respect to the behavior of integral bridges is presented.

Comparison between the two major forms for highway bridges, integral (or jointless) versus jointed, has shown that the former present several important advantages, including reduced construction and maintenance cost, as a result of elimination of joints. This is because bridge joints are expensive to purchase and install, and continuous maintenance is needed to keep them working properly (*1*).

The first integral bridges were designed after 1956. At the beginning, they were short in length and designed with precautions. Until 1985, the maximum length for integral concrete bridges had increased to 282 m and for those with steel superstructure to 127 m. In Tennessee it has become policy that "all bridges shall be continuous from end to end, and there shall be no intermediate joints introduced in the bridge deck other than cold joints required for construction" (*2*).

Bridges are subjected to various loading conditions, such as self-weight, temperature, and creep. The stresses caused by such loadings result in different total stresses for the jointed and the integral bridges. For example, a simply supported bridge develops higher stresses at midspan than does an indeterminate frame-type structure caused by dead and live loads, whereas stresses caused by thermal expansion or contraction in a simply supported bridge are much smaller (if at all) than those developed in the indeterminate system.

Several integral bridges have been built during the last few years in many states. Nevertheless, there is still no final and complete answer to what makes those bridges work efficiently and survive the high stresses that are supposed to develop. In a comparison of integral and jointed bridges Siros and Spyrakos (*3*) have shown that the change of bending moments because of creep in an integral bridge can be up to three times smaller than that in a jointed bridge. This fact, possibly being part of the answer, was the motivation for further investigation of creep stresses that develop in an indeterminate composite bridge.

A three-dimensional (3-D) model was developed and the rate of creep method (RCM) formulation was utilized in a step-by-step computer analysis. The age-adjusted effective modulus method (AEMM) was also used in a linear two-dimensional (2-D) analysis. Stresses at the top of the concrete slab and at the bottom of the steel stringer were calculated for several critical points along the bridges. Stress versus time plots are shown, and comparisons are presented between the 3-D and the 2-D analysis.

Department of Civil Engineering, Constructed Facilities Center, West Virginia University, Morgantown, W.Va. 26505-6103.

STRESS-STRAIN RELATIONSHIP

A concrete member that is subjected to a constant load exhibits continuous change of strain over time at each point because of creep. The creep law that describes this behavior is a function of time, strength of the material, and stress at each time.

One of the most widely accepted methods (*4*) for the calculation of creep in concrete, the RCM, is utilized here for the 3-D analysis. This method is mathematically attractive because it formulates the creep problem as a simple first-order differential equation, and therefore a step-by-step analysis can be easily carried out.

Gilbert (*5*) has utilized both the RCM and the AEMM to calculate creep stresses for a composite cross section, when the internal forces acting on the section at a certain time are known. When the structure is indeterminate, however, creep causes change of the reactions and the internal forces in the structure with time. Ghali (*6*) presents a methodology for 2-D creep analysis of indeterminate structures, which is also employed here for the 2-D analysis.

Bazant (*7*) discusses the multiaxial stress case for the AEMM. The analysis of bridges as 3-D structures is performed with the RCM. The formulation as it is given in the literature cannot be used directly with FEM analysis packages, and therefore a conversion is required.

In finite element analysis, the 3-D state of stress is taken into account by calculating the equivalent total strain at each time step as follows (*8*):

$$\varepsilon_{el} = \frac{1}{(1+\nu)\sqrt{2}}\left[\left(\varepsilon_x-\varepsilon_y\right)^2+\left(\varepsilon_y-\varepsilon_x\right)^2+\left(\varepsilon_z-\varepsilon_x\right)^2+\frac{3}{2}\left(\gamma_{xy}\right)^2+\frac{3}{2}\left(\gamma_{yz}\right)^2+\frac{3}{2}\left(\gamma_{zx}\right)^2\right]^{1/2} \quad (1)$$

where ε_x, ε_y, and ε_z are the axial strains in the x, y, and z directions, respectively, and γ_{xy}, γ_{yz}, γ_{zx} are shear strains in the respective planes and directions.

According to the RCM, the rate of creep strain at time t is a function of the stress, $\sigma(t)$, the creep coefficient derivative, $\phi'(t,t_o)$, and the modulus of elasticity of concrete at the present time, $E_c(t_o)$, that is

$$\varepsilon'_{cr}(t,t_o) = \phi'(t,t_o)\frac{\sigma(t)}{E_c(t_o)} \quad (2)$$

In this creep formulation, the aging of the concrete is ignored. Therefore creep may be overestimated for old concrete, but when the load starts acting soon after casting the concrete, the method gives good results.

The modulus of elasticity $E_c(t)$ of concrete varies also with time according to Equation 3 but should be taken as constant equal to $E(28)$ to arrive at a procedure that is computationally manageable. Note that in 28 days the concrete has gained about 90 percent of its strength. $E_c(t)$ is computed from

$$E_c(t) = E(28)\sqrt{\frac{t}{(4 + 0.85t)}} \tag{3}$$

The American Concrete Institute (*9*) Committee 209 suggests that $\phi(t)$ for $t_o = 7$ days be taken as

$$\phi(t) = \phi_u\left[\frac{t^{0.6}}{10 + t^{0.6}}\right] \tag{4}$$

with $\phi_u = 2.35g_c$ and $g_c = g_{la}\, g_h\, g_{vs}$

where g_{la}, g_h, and g_{vs} are constants that depend on age of loading, humidity, and ratio of volume to surface of the member, respectively. For constant humidity of 40 percent, age of loading of 7 days, and ratio of volume to surface of 1.5, g_c is equal to 1 For practical applications the estimation of this factor involves many uncertainties because humidity and temperature in the air change continuously with time.

NONLINEAR ANALYSIS

The analysis starts with the application of the self-weight or any equivalent sustained load on the structure. The time of application of the load t_o is assumed to be at 7 days. The duration of the loading is taken as 100,000 days. This time is required until the creep coefficient reaches the assumed ultimate value $\phi_u = 2.5$.

According to Equation 4, $\phi = 2.4$ for $t = 10{,}000$ and $\phi = 2.475$ for $t = 100{,}000$. From Figure 1 it is clear that the change of ϕ after the 100,000 days is slow and therefore the predicted creep will be small. From the same figure it can be seen that the change of strain is fast during the first 500 days and consequently a small time step is needed for the first period to reach convergence.

In finite element analysis, the creep formulation is based on the constitutive law (*10*):

$$\varepsilon'_{cr} = c_1\sigma^{c_2}t^{c_3} \tag{5a}$$

where c_1, c_2, and c_3 are constants. Therefore, Equation 2, corresponding to the RCM, must be converted into this form.

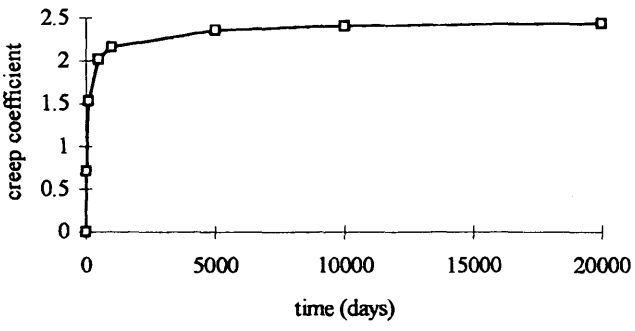

FIGURE 1 Creep coefficient versus time.

For each interval, as defined between the squares in Figure 1, Equation 4 can be expressed as

$$\phi = at^N \tag{5b}$$

where a and N are constants calculated by linear regression analysis (*11*). The constants N and a depend on the duration of each interval, which should be small enough so that the coefficient of variation r^2 is close to 1 (*12*).

The first derivative of this equation with respect to time is given by

$$\phi' = Nat^{N-1} \tag{6}$$

Substituting Equation 6 into Equation 2 the following is obtained:

$$\varepsilon'_{cr}(t,t_o) = \frac{\sigma(t)}{E_c(t_o)}\, Nat^{N-1} \tag{7}$$

or

$$\varepsilon'_{cr}(t,t_o) = \frac{Na}{E_c(t_o)}\, \sigma(t)t^{N-1} \tag{8}$$

and finally,

$$\varepsilon'_{cr} = c_1\sigma^{c_2}t^{c_3} \tag{9}$$

where

$$c_1 = \frac{Na}{E_c(t_o)} \qquad c_2 = 1 \qquad c_3 = N - 1 \tag{10}$$

The constants c_1, c_2, and c_3 describe the creep low for a given ϕ, t_o, and $E_c(t_o)$ and can be incorporated into well-documented finite element analysis programs such as ANSYS (*13*) and ABACUS (*14*).

The creep strain increment $\Delta\varepsilon_{cr} = \varepsilon'_{cr} * \Delta t$ is then calculated and added to the elastic strain. The new stress level is calculated at each point, and the procedure is repeated by calculating the next creep strain change. At each step the $\Delta\varepsilon_{cr}/\varepsilon_{ei}$ is calculated and the time step size is increased when the ratio is smaller than a predefined criterion, which for most practical applications can be taken as 0.25 (*8*). During the initial period though, when the creep strain rate is high, this ratio should be kept below 0.10 by increasing the number of iterations or decreasing the time step size.

THREE-DIMENSIONAL ANALYSIS

In the process of developing the 3-D model, many modeling aspects were considered, such as size and aspect ratio of elements, and combination of various types of elements (*15*). The model utilizes four node isoparametric plate elements with 6 degrees of freedom (dof) per node to simulate the concrete deck and the bridge abutments. Beam elements with six dof per node model the steel stringers and are connected to the plate elements of the slab with small and stiff fictitious beam elements (Figure 2). Close to the abutments and intermediate supports, more elements are used as a result of the anticipated higher stress gradient. At those regions, triangular elements are also used for gradual element size increase. A model with the minimum number of elements is essential in nonlinear analysis because of the substantial processing time. Therefore modeling

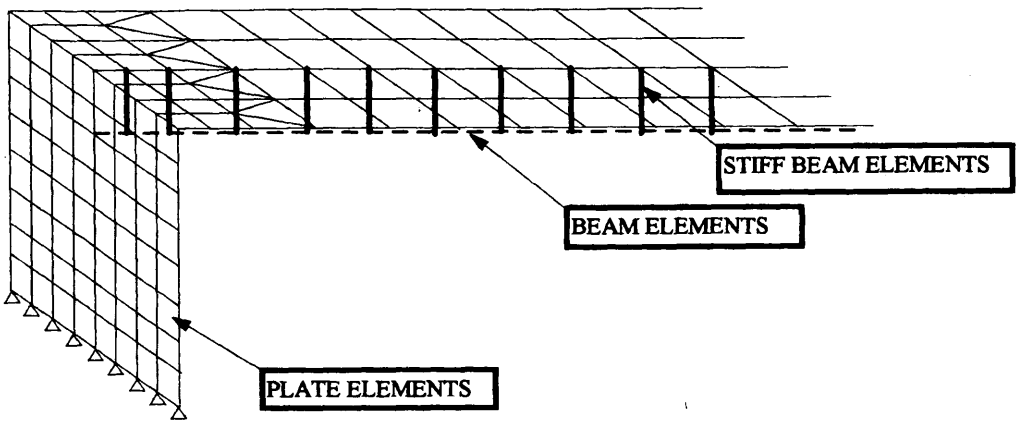

FIGURE 2 Detail of the 3-D model: abutment and deck.

rules and various alternative modeling schemes were employed toward this goal with minimum loss of computational accuracy. The number of the stiff fictitious connectors as well as their stiffness had to be kept at a minimum to avoid numerical instability. The size of the elements was also properly chosen at each point to satisfy size and aspect ratio requirements. A detailed discussion of the modeling considerations is given by Spyrakos (*16*). Special emphasis has been given to proper modeling of the boundary conditions. Simulation of the boundary conditions that is not accurate may result in small errors in a linear analysis. However, in nonlinear analysis caused by the multiple steps the error is accumulated.

A small creep (practically 0) was given for the time 0 to 7 days because nonzero values are required by the iterative algorithm.

The ultimate creep coefficient varies from 1.35 to 4.15 (*9*), but for most practical applications it ranges from 2 to 2.5. The aging coefficient (χ) varies from 0.774 to 0.8 for $\phi = 2.5$ and variable E_c and from 0.839 to 0.899 for constant E_c (*7*).

EXAMPLES

Example 1

A single-span bridge is analyzed first. Figure 3 shows the geometry of the structure. The material and geometric properties corresponding to one stringer are given as follows:

Steel:
E_{st} = 200 GPa I_{st} = 0.00278 m^4 A_{st} = 0.02806 m^2

Concrete:
E_c = 30 GPa I_{ocol} = 0.03487 m^4 Abutment thickness = 0.5677 m

$\phi(\infty,7)$ = 2.5 $\chi(\infty,7)$ = 0.8 Self-weight = 18919 N/m

The 2-D analysis is carried out according to Ghali and Favre (*6*), and the results are shown in Table 1. Results from the 3-D analysis are shown in Figure 4*a* and *b*. Stresses are calculated at midspan and the end of the deck. Negative stresses are compressive, whereas positive ones are tensile.

Example 2

The second example is a two-span bridge built in Iowa. The middle support is simulated here as a hinge. The total self-weight of the structure per stringer is 21 315 N/m. The dimensions and the geometry of the bridge are shown in Figure 5. The material and geometric properties are as follows:

E_{st} = 200 GPa I_{st} = 0.008625 m^4 A_{st} = 0.03129 m^4

E_c = 23.255 GPa I_{col} = 0.28525 m^4 Abutment thickness = 1.0668 m

$\phi(\infty,7)$ = 2.5 $\chi(\infty,7)$ = 0.8 Self-weight = 21 315 N/m

Results for three sections are listed for the first span of the bridge, the end of the deck, the midspan, and the center of the bridge (hinge location). Because the structure is symmetric the results are identical for the second span (see Figure 6 and Table 2).

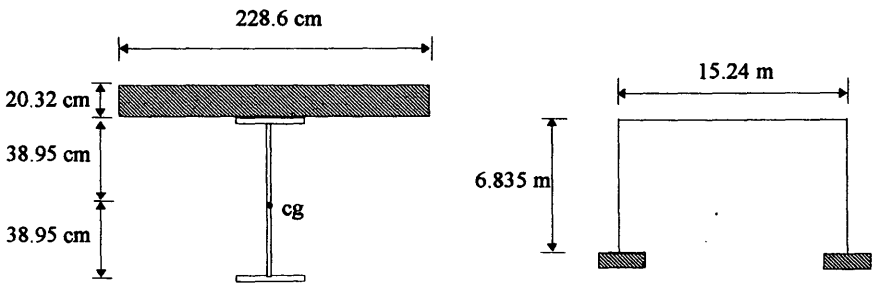

FIGURE 3 Geometry of the single-span bridge.

TABLE 1 Creep Analysis for Single-Span Bridge: 2-D versus 3-D

LOCATION	CREEP 2D (MPa)	CREEP 3D (MPa)	DIFFER. (MPa)	DIFFER. (%)
TOP OF CONCRETE				
ABUTMENT	-0.4207	-0.5724	0.1517	26
MIDSPAN	0.6138	0.6965	0.0827	12
BOTTOM OF STEEL				
ABUTMENT	-5.6827	-5.4689	0.2138	4
MIDSPAN	0.4483	0.5931	0.1448	24

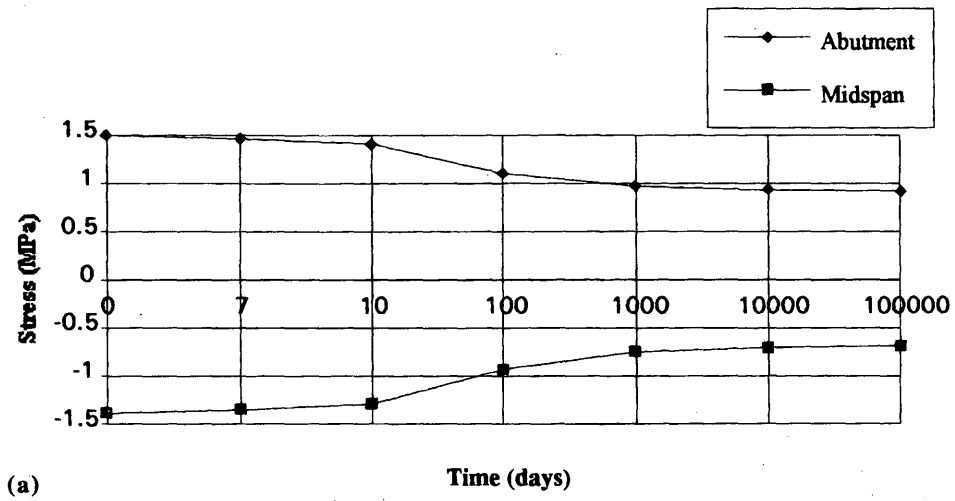

(a)

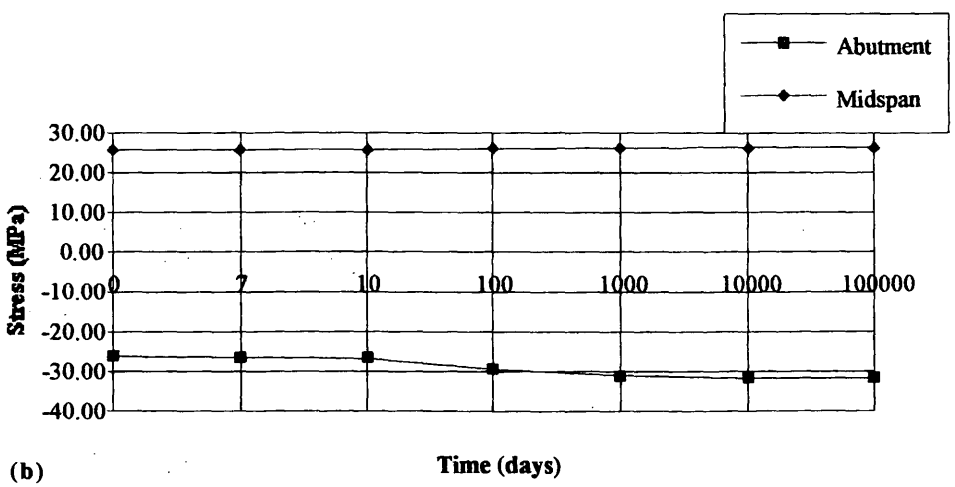

(b)

FIGURE 4 Stresses versus time, single-span bridge: (*a*) at the top of the concrete slab; (*b*) at the bottom of the steel beam.

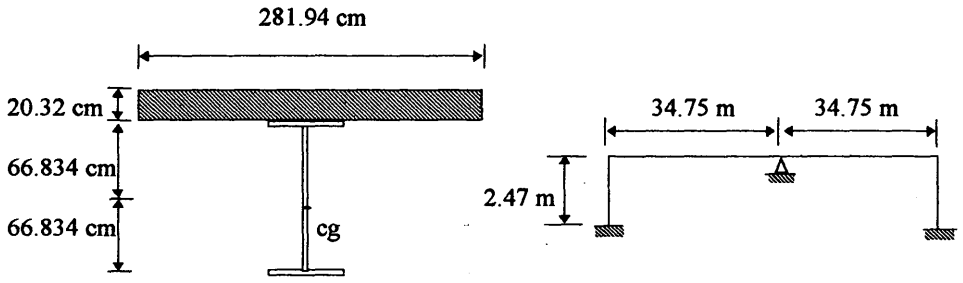

FIGURE 5 Geometry of the two-span bridge.

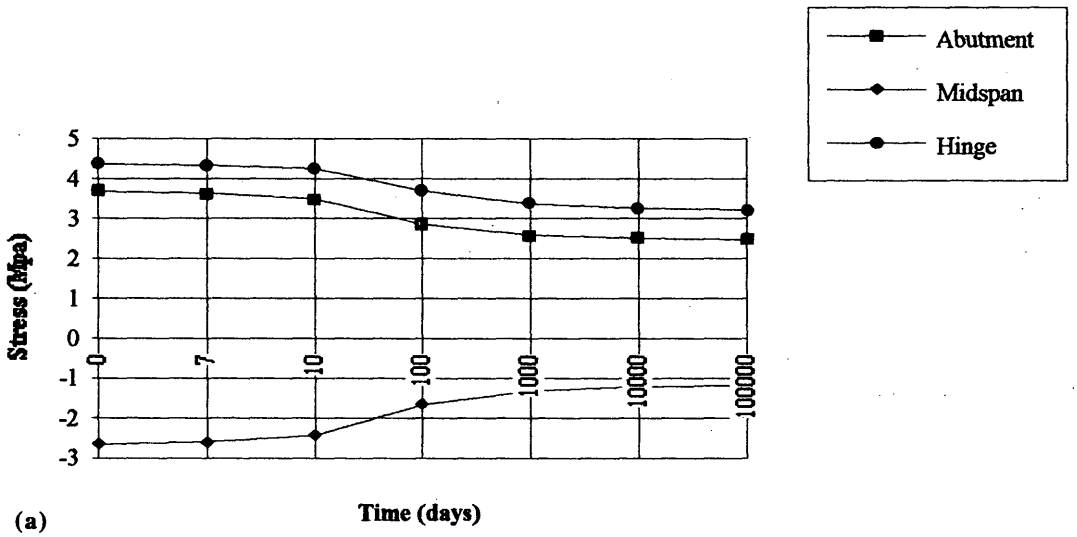

(a)

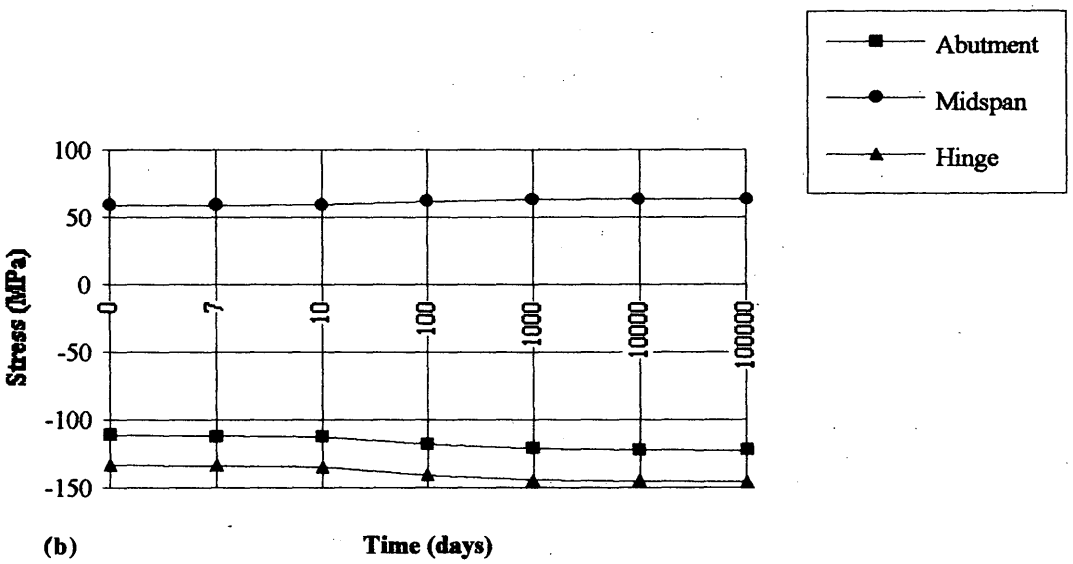

(b)

FIGURE 6 Stresses versus time, two-span bridge (*a*) at the top of the concrete slab; (*b*) at the bottom of the steel beam.

TABLE 2 Creep Analysis for Two-Span Bridge: 2-D versus 3-D

LOCATION	CREEP 2D (MPa)	CREEP 3D (MPa)	DIFFER. (MPa)	DIFFER. (%)
TOP OF CONCRETE				
ABUTMENT	-0.9724	-1.2000	0.2276	19
MIDSPAN	1.1655	1.4552	0.2897	20
HINGE	-1.3379	-1.1517	0.1862	14
BOTTOM OF STEEL				
ABUTMENT	-13.3034	-11.3172	1.9862	15
MIDSPAN	6.0620	5.1103	0.9517	16
HINGE	-12.4414	-12.3517	0.0897	1

RESULTS AND DISCUSSION

Two indeterminate composite structural systems are analyzed for creep: a single-span bridge (15.24 m) and a two-span bridge (2 × 34.75 m). The geometric and material properties are varied. Static and creep analysis are carried out with 2-D and 3-D models. Two creep analysis methods are used: the RCM and the AEMM. For the nonlinear analysis with the 3-D models the time step is varied. At the beginning, when creep was large, the step was small but was increased with time.

Tables 1 and 2 show that despite the various approaches used (RCM and AEMM), the differences between the 3-D and 2-D analysis range from 4 to 26 percent for the first example and from 15 to 20 percent for the second example. Usually the concrete stresses show higher differences because the comparison is between small numbers. From the results it is obvious that when the high stresses of steel are compared, the difference in percentage is smaller.

Results from 3-D analysis are not always smaller than those from the 2-D analysis. Tables 3 and 4 show the relative significance of creep with respect to dead load stresses. Creep stresses in concrete are as high as 26 to 55 percent of the dead load stresses and in steel creep stresses are as high as 2 to 21 percent.

In bridge design, dead load, live load, differential settlements, temperature, shrinkage, creep, and other effects are considered. It is understood that a fraction of the allowable stress of the material should be assumed to withstand the creep stresses. Therefore, a comparison of the creep stresses with the allowable stresses of steel and concrete provide an insight into how important creep is for jointless bridges. The creep stresses are only 1 to 9 percent of the allowable for the steel and 3 to 42 percent for the concrete (Tables

TABLE 3 Relative Significance of Creep With Respect To Dead Load Stresses: Single-Span Bridge

LOCATION	DEAD LOAD 3D (MPa)	CREEP 3D (MPa)	CREEP/DL (%)
TOP OF CONCRETE			
ABUTMENT	1.4965	-0.5724	38
MIDSPAN	-1.4069	0.6965	49
BOTTOM OF STEEL			
ABUTMENT	-26.3586	-5.4689	21
MIDSPAN	25.6689	0.5931	2

TABLE 4 Relative Significance of Creep With Respect To Dead Load Stresses; Two-Span Bridge

LOCATION	DEAD LOAD 3D (MPa)	CREEP 3D (MPa)	CREEP/DL (%)
TOP OF CONCRETE			
ABUTMENT	3.6827	-1.2000	32
MIDSPAN	-2.6483	1.4551	55
HINGE	4.3724	-1.1517	26
BOTTOM OF STEEL			
ABUTMENT	-111.1448	-11.3172	10
MIDSPAN	58.9724	5.1103	9
HINGE	-133.1931	-12.3517	9

5 and 6). It is clear that the steel stresses caused by creep are insignificant, but the concrete stresses can be large. Notice though that the concrete stresses decrease as a result of creep.

As discussed by Siros and Spyrakos (*3*), the moment change caused by creep is negative at all points along the deck, which implies that negative moments (supports) as a result of dead load will increase, but positive moments (midspans) will decrease. This was further verified with the present work, although moments are not shown but rather stresses are presented in the tables and figures. Also, the axial forces caused by creep should not be overlooked because they contribute to the formation of the total stresses at each point.

The results in Tables 1 and 2 demonstrate that stresses at the bottom of the steel stringers increase as a result of creep, but stresses at the top of the concrete slab decrease. It should be noticed that this happens at all points along the superstructure—for example at points of negative moment (support) and at points of positive moment (midspan).

Consequently, we can summarize that creep is additive to the dead load effect for the bottom of the steel but is acting beneficially at the top of the concrete by reducing both negative and positive stresses. Sometimes, however, the reduction of negative (compressive) stresses can be large enough to even change the sign and eventually produce tensile stresses (*17*). In such cases reinforcing of the top surface of the concrete deck would be necessary. Even though creep stress in concrete can be as high as 49 percent of the dead load stress and theoretically may cause reversal of the sign of the initial stress, it has not been observed in the analysis of several bridges of various span lengths and geometries (*18*).

SUMMARY AND CONCLUSIONS

Three-dimensional and two-dimensional analyses are performed to assess the creep effect on hybrid bridges with integral abutments. Two typical bridges with different dimensions and geometric and material properties are analyzed. Creep stresses at the top of the concrete slab and the bottom of the steel stringer are calculated for various ages with a 3-D nonlinear analysis. The results can be summarized as follows:

1. The two types of analysis (2-D and 3-D) arrived at results that differ by 1 to 29 percent. Comparisons of steel stresses usually show smaller differences (1 to 24 percent) than do concrete stresses (11 to 29 percent).
2. Creep stresses as a fraction of the dead load stresses range from 2 to 21 percent for the steel and 26 to 49 percent for the concrete.
3. Compared with the allowable stresses of the materials, creep stresses consist of 1 to 9 percent for steel and 3 to 42 percent for concrete.
4. Creep causes a small increase in positive and negative stresses at the bottom of steel stringers and a reduction in the tensile and compressive stresses at the top of the concrete deck. Designers should be alert because such reduction of compressive stresses may reverse them to tensile, in which case steel reinforcement is necessary.

ACKNOWLEDGMENT

This work is sponsored by the West Virginia Department of Highways and FHWA.

TABLE 5 Creep Stresses Versus Allowable Stress of Each Material: Single-Span Bridge

LOCATION	CREEP 3D (MPa)	ALLOWABLE (MPa)	CREEP/ALL. (%)
TOP OF CONCRETE			
ABUTMENT	-0.5724	3.6827	16
MIDSPAN	0.6965	18.0689	4
BOTTOM OF STEEL			
ABUTMENT	-5.4689	140	4
MIDSPAN	0.5931	140	1

TABLE 6 Creep Stresses Versus Allowable Stress of Each Material: Two-Span Bridge

LOCATION	CREEP 3D (MPa)	ALLOWABLE (MPa)	CREEP/ALL. (%)
TOP OF CONCRETE			
ABUTMENT	-1.2000	2.8552	42
MIDSPAN	1.4552	10.8621	13
HINGE	-1.1517	2.8552	40
BOTTOM OF STEEL			
ABUTMENT	-11.3172	140	8
MIDSPAN	5.1103	140	4
HINGE	-12.3517	140	9

REFERENCES

1. Wasserman, E. P. Jointless Bridge Deck. *Engineering Journal*/AISC, 3rd Quarter, 1987.
2. Loveall, C. L. Jointless Bridge Decks. *Civil Engineering*, Nov. 1985.
3. Siros, D. A., and C. C. Spyrakos. A Study of Jointless Bridge Behavior. Proc., 12th Structures Congress, Atlanta, Ga., Vol. 1, ASCE April 1994, pp. 485–490.
4. Bazant, Z. P. Comparison of Approximate Linear Methods for Concrete Creep. *Journal of the Structural Division*, ASCE, Vol. 99, Sept. 1973, pp. 1851–1874.
5. Gilbert, I. R. Time-Dependent Analysis of Composite Steel-Concrete Sections. *Journal of Structural Engineering*, ASCE, Vol. 115, No. 11, Nov. 1989, pp. 2687–2705.
6. Ghali, A., and R. Favre. *Concrete Structures: Stresses and Deformations*. Chapman and Hall, London, 1986.
7. Bazant, Z. P. Prediction of Concrete Creep Effects Using Age-Adjusted Effective Modulus Method. *ACI Journal*, Vol. 69, April 1972, pp. 212–217.
8. *Theoretical Manual Volume*, Revision 4.4. ANSYS.
9. Prediction of Creep, Shrinkage and Temperature Effects in Concrete Structures, In *Manual of Concrete Practice*. American Concrete Institute, 1988. pp. 209R-1-209R-60.
10. Bathe, K. J. *Finite Elements Procedures in Engineering Analysis*. Prentice-Hall, Englewood, N.J. 1982.
11. Walker, R. D. Numerical Methods for Engineers and Scientists. TAB Professional and Reference Books, 1st ed., 1987, pp. 245–251.
12. Meyer, S. L. Data Analysis for Scientists and Engineers. Wiley, 1975.
13. *ANSYS User's Manual*, Vol. 1, Revision 4.4.
14. *ABAQUS Standard User's Manual, version 5.3*. Sections 4.6.9 and 7.6.9, 1993.
15. *ALGOR User's Manual*, 1994.
16. Spyrakos, C. C. *Finite Element Modeling in Engineering Practice*. West Virginia University Press, Morgantown, 1994.
17. McHenry, D. A New Aspect of Creep in Concrete and its Applications to Design. *Proc., ASTM*, Vol. 43, 1943, pp. 1069–1086.
18. Siros, K. A. *Three Dimensional Analysis of Integral Bridges—Loading and Behavior*. Dissertation, West Virginia University, Morgantown, 1995.

Publication of this paper sponsored by Committee on Dynamics and Field Testing of Bridges.